MODELING OF PHASE SPECTRUM TO SIMULATE DESIGN GROUND MOTIONS

Juin-Fu Chai* and Chin-Hsiung Loh
National Center for Research on Earthquake Engineering
Taipei, Taiwan 106, R.O.C.

Tadanobu Sato
Disaster Prevention Research Institute
Kyoto University
Kyoto, Japan

Key Words: phase spectrum, group delay time, design response spectrum, Kalman filtering.

ABSTRACT

In this paper, the concept of group delay time is used to model the phase spectrum on each separated frequency range according to the compact support of Meyer wavelet. The regression equations to predict the mean value and standard deviation of group delay times can be developed on the basis of the recorded earthquake set. Based on the predicted mean value and standard deviation for a target site, the sample of group delay time at a certain discrete frequency can be either generated randomly by a specified probability density function or simulated conditionally by applying the Kalman filtering technique to consist of the earthquake data observed at nearby stations. Then, the phase spectrum can be modeled by integrating the simulated group delay times. On the basis of the modeled phase spectrum, the design ground motion can be simulated by the iteration process of modifying the Fourier amplitude, such that the associated spectral response acceleration will be compatible with the design response spectrum as specified by the seismic design code.

I. INTRODUCTION

In recent years, time history analysis has become more and more important for the seismic design of structures, and hence, it is required to develop a simulation method to simulate the time history of design ground motion. For a site of interest, the appropriate design ground motions should be not only compatible with the design response spectrum as specified by the seismic design code, but also consistent with the earthquake data observed at the target site to perform the same waveform characteristics.

A primitive method to simulate design ground motions is to generate a nonstationary time history by multiplying an envelope function (Jennings, *et al.*, 1968) to a stationary time history simulated by using random phase criteria (Shinozuka and Jan, 1972). However, it may lose the waveform characteristics of the target site. Another method is to use the phase spectrum of an observed ground motion to control the non-stationary nature of earthquake motions. Consider the 1999 Chi-Chi earthquake (Taiwan), the

*Correspondence addressee

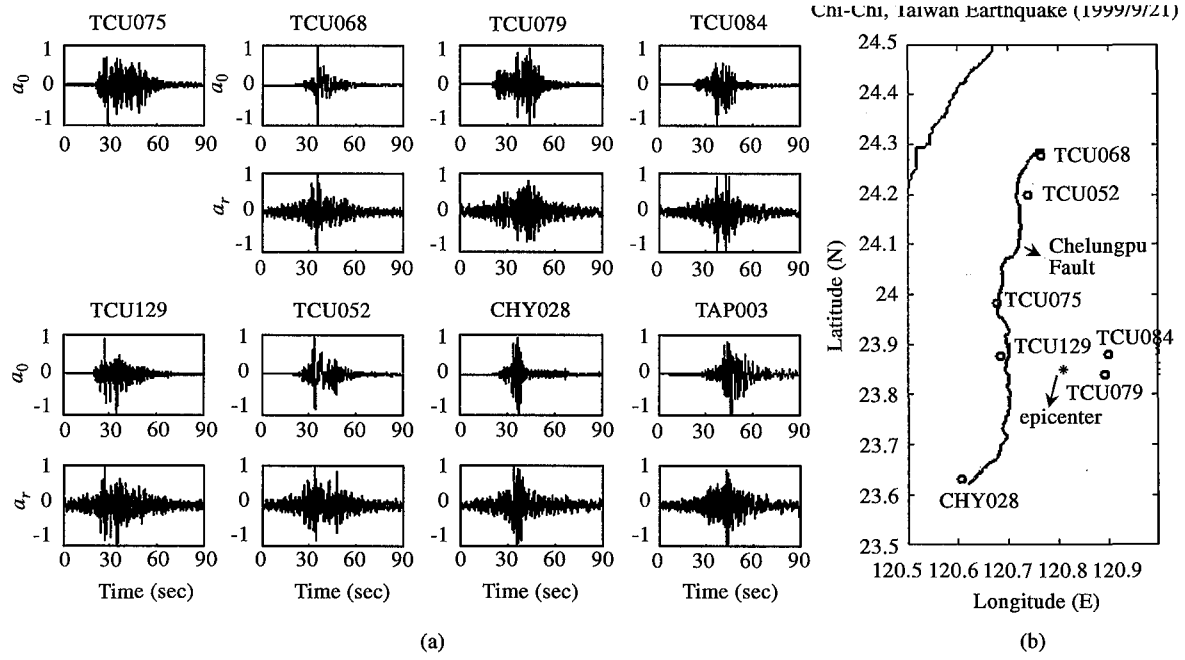

Fig. 1 (a) Comparison of the observed seismograms (a_0) and the time histories (a_r) recovered by their own phase spectra and the Fourier amplitude determined at the reference site CHY075, and (b) Locations of the reference site and other observation stations

ground motions observed at some stations near the Chelungpu Fault and the epicenter are shown in Fig. 1(a) as denoted by a_0, and Fig. 1(b) shows the locations of these stations. For each observed ground motion, we can obtain the phase spectrum and the Fourier amplitude. Defining station TCU075 as a reference site, and for any other site, based on its own phase spectrum and the common Fourier amplitude determined at the reference site, a new time history can be recovered and shown in Fig. 1(a) as denoted by a_r. It can be found that, although the Fourier amplitude has been changed, the recovered waveform is very similar to the original one, because they share the same phase spectrum. Furthermore, as shown in Fig. 1(a), the similar waveform can be also recovered for the case of station TAP003, even though the station is located in the Taipei Basin, 200 km away from the reference site (TCU075). It implies that the most important issue for simulating the design ground motion is to model the phase spectrum. As long as the phase spectrum for a site of interest is modeled, we can simulate the design ground motion by modifying the Fourier amplitude based on the available design response spectrum. Hence, the simulated design ground motion will be compatible with the design response spectrum and also perform the same waveform characteristics as the earthquake ground motions observed at the target site. Because the phase characteristic of earthquake motion strongly controls the non-stationary nature of earthquake motions, many methodologies have been developed to model the phase spectrum of ground motions (Sato *et al.*, 1998 and Sato *et al.*, 1999).

Group delay time is defined as the derivative of the phase spectrum with respect to circular frequency (Papoulis, 1962). The mean value of group delay time and its standard deviation within a certain frequency range represent the central arrival time and duration, respectively, of the earthquake motion with frequency content of such a bandwidth (Satoh *et al.*, 1996). Therefore, it is much easier to model the group delay time than to model the phase spectrum directly. Furthermore, in order to simulate better ground motions, the phase spectrum should be modeled one by one for a series of separate frequency bands, rather than once for the whole frequency range, and it is implemented by wavelet decomposition. In this paper, the discrete Meyer wavelet decomposition (Meyer, 1989) is adopted because the Meyer wavelet is a frequency band-limited function whose Fourier transformation is smooth, and hence it provides a much faster asymptotic decay in the time domain. Furthermore, the discrete Meyer wavelet transformation of observed ground motions is determined easily in the real domain. The procedure to determine the group delay time and the associated mean value and standard deviation for each decomposed component of an observed ground motion is illustrated briefly in this paper.

On the other hand, based on statistical analysis, it can be found that the student t-distribution with a degree of freedom ϕ=3 can be recognized as the

representative distribution of group delay times within the compact support of Meyer wavelet. Therefore, for the given mean value and standard deviation of group delay times of a certain decomposed component, the sample of group delay times at each discrete frequency within the associated compact support can be generated randomly by the identified probability density function of student t-distribution (ϕ=3).

In general, the mean value and standard deviation of group delay times of each decomposed component can be modeled as functions of the epicentral distance and earthquake magnitude. However, because the object of this study is to determine the design ground motion according to the Chi-Chi earthquake at a site with no records available, the dependence of the earthquake magnitude is dropped. On the basis of the recorded data from the observation stations during the Chi-Chi earthquake, the attenuation relations to predict the mean value and standard deviation of group delay times of each component can be regressed as functions of the hypocentral distance in this paper.

For a site of interest, in addition to the random generation of group delay times by only the predicted mean value and standard deviation, the earthquake data observed at nearby stations can be considered together to simulate a sample of group delay time by applying conditional simulation methods. Conditional simulation methods should be devised to allow the realization of a sample field at an unobserved location, which satisfies the properties of a stochastic field and is compatible with measured values at observed locations. Nonstochastic conditional simulation (Kameda and Morikawa, 1992), application of the Kriging method (Vanmarck and Fenton, 1991; Hoshiya and Murayama, 1993), and Kalman filtering technique (Sato and Imabayashi, 1999) were developed by using the cross-spectrum to model spatial stochastic characteristics of ground motions. In this paper, after defining a spatial correlation of group delay times, the Kalman filtering technique is applied to model the group delay times and further to simulate the phase spectrum for an unobserved point.

Finally, based on the predicted phase spectrum at a site of interest, the design ground motion can be simulated by modifying the Fourier amplitude owing to the resonance effect, such that the associated spectral response acceleration will be compatible with the design response spectrum as specified by the seismic design code. Because of the nonstationary nature included in the modeled phase spectrum, this simulated design ground motion will perform the same waveform characteristics as the earthquake ground motions observed at the target site.

II. DETERMINATION OF GROUP DELAY TIME

Group delay time $t_{gr}(\omega)$ is defined as the derivative of the phase spectrum $\Phi(\omega)$ with respect to circular frequency ω.

$$t_{gr}(\omega) = \frac{d\Phi(\omega)}{d\omega} \tag{1}$$

The phase spectrum determined from a ground motion should be unwrapped to obtain the group delay times. The mean value and standard deviation of group delay times within a certain frequency range express the central arrival time and duration, respectively, of the earthquake motion with frequency content of such a bandwidth.

In this study, based on the prediction of group delay times for a series of separate frequency bands, the phase spectrum will be simulated within a certain frequency range one by one, rather than once for the whole frequency range. It is implemented by using the Meyer wavelet decomposition. The Meyer wavelet function $\varphi(t)$ is defined explicitly in the frequency domain by

$$\overline{\varphi}(f) = \begin{cases} 0 & ; |f| \notin [1/3, 4/3] \\ e^{i\pi f}\sin[\frac{\pi}{2}\beta(3|f|-1)] & ; 1/3 \le |f| \le 2/3 \\ e^{i\pi f}\cos[\frac{\pi}{2}\beta(\frac{3}{2}|f|-1)] & ; 2/3 \le |f| \le 4/3 \end{cases} \tag{2}$$

where $\overline{\varphi}(f)$ is the Fourier transformation of $\varphi(t)$, and $\beta(\alpha)$ is an auxiliary function that goes from 0 to 1 on the interval [0,1] and can be defined by (Daubechies, 1992)

$$\beta(\alpha)=a^4(35-84\alpha+70\alpha^2-20\alpha^3);\ a\in[0,1] \tag{3}$$

It can be found that the Meyer wavelet is a frequency band-limited function whose Fourier transformation is smooth, and hence it provides a much faster asymptotic decay in the time domain. The Meyer wavelet $\varphi(t)$ and its Fourier amplitude $|\overline{\varphi}(f)|$ are illustrated in Fig. 2.

The discrete wavelet transformation of a time function $x(t)$ and its inverse transformation are defined by

$$x(t) = \sum_j x_j(t) = \sum_j (\sum_k a_{jk}\varphi_{jk}(t))$$

$$\varphi_{jk}(t) = 2^{j/2}\varphi(2^j t - k)$$

$$a_{jk} = \int_{-\infty}^{\infty} \varphi_{jk}(t)x(t)dt \tag{4}$$

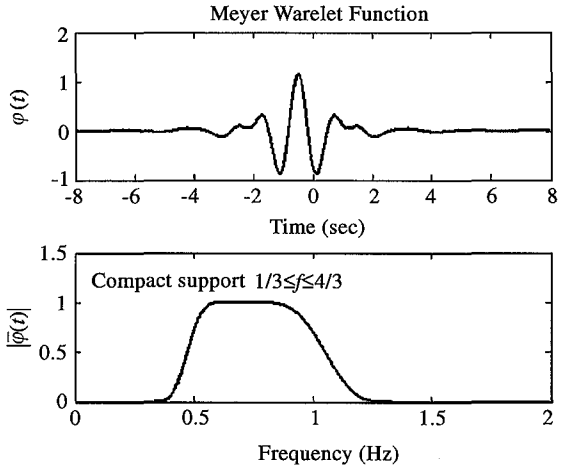

Fig. 2 Meyer wavelet $\varphi(t)$ and its Fourier amplitude $|\overline{\varphi}(f)|$

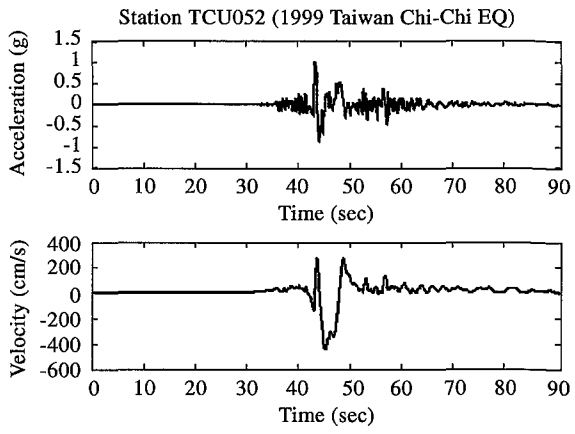

Fig. 3 Ground motion observed at station TCU052 during the Chi-Chi earthquake (1999)

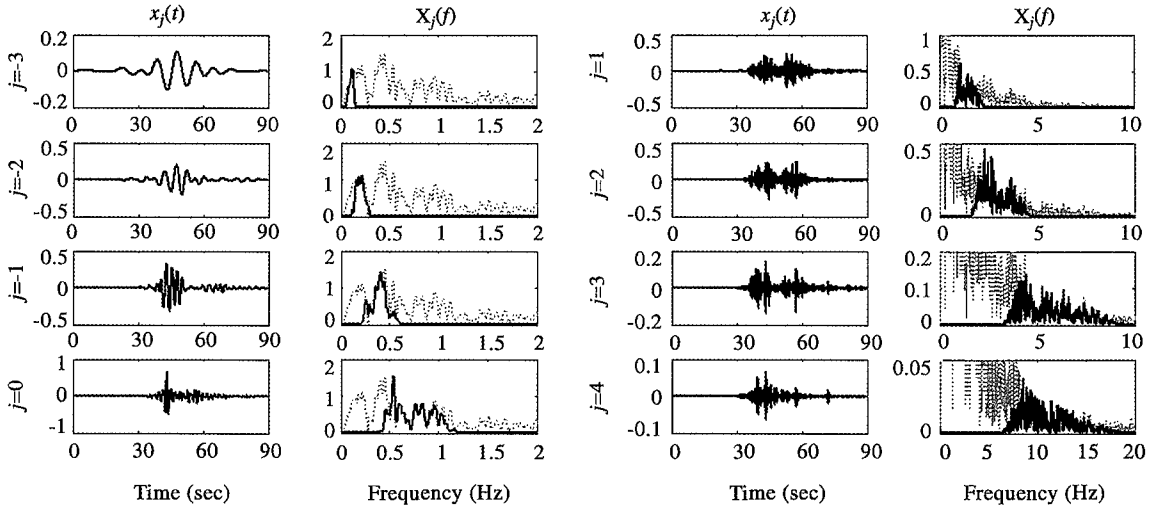

Fig. 4 Time histories and Fourier amplitude spectra of the Meyer wavelet decomposed components (j=-3~4) of the ground motion observed at station TCU052

where $\varphi_{jk}(t)$ is the discrete Meyer wavelet function with integers j and k denoting the scale factor and time shift, respectively, and the set of functions $\varphi_{jk}(t)$ for all scales is an orthonormal basis for the linear space of $L_2(R)$. Owing to the Meyer wavelet transformation, all components $x_j(t)$ with different scale factors, j, are orthogonal to each other, and the Fourier transformation of the j-th component $X_j(f)$ has a compact support defined by $2^j/3 \le f \le 2^{j+2}/3$. It is noted that adjacent compact supports overlap with each other in the frequency domain.

We consider the earthquake data observed at station TCU052 during the Chi-Chi earthquake as an example. As shown in Fig. 3, it is a typical near-fault ground motion, and for convenience, the value of PGA has been scaled to become 1g. Based on Eq. (4), the orthogonal components can be decomposed by means of the Meyer wavelet transformation. Both the time histories and the Fourier amplitude spectra of the components with scale factor j=-3 to 4 are shown in Fig. 4. It is found that the signals in a component with smaller scale factor (lower frequency contents) concentrate to become a single group with only one central arrival time. However, the signals in a component with a larger scale factor (higher frequency contents) separate to many groups and arrive at different times. It may be due to the larger bandwidth of frequency contents, the crack open and healing processes of the fault rupture, and may even be caused by sub-events. The overlap situation can be observed in the Fourier amplitude spectrum, and further, the Fourier amplitude at the central frequency range on each compact support is coincident with the one determined from the total ground motion (denoted

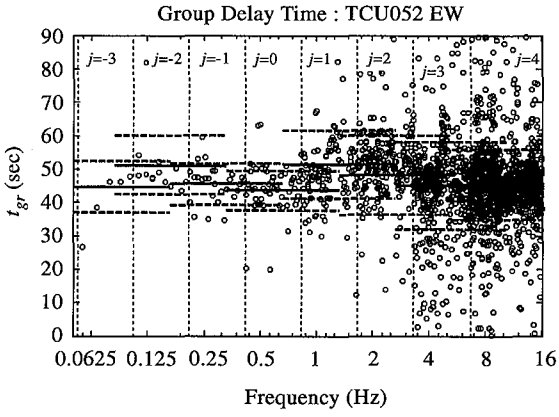

Fig. 5 Distribution of the group delay time for the decomposed components with j=-3 to 4 of the ground motion observed at station TCU052

by a dashed line). On the other hand, based on the Fourier spectrum of the total ground motion, it can be found that the Fourier amplitudes for frequencies higher than 20 Hz are much smaller than those for lower frequencies. Hence, signals with frequencies higher than 20 Hz are ignored, and only the components with scale factor j=-3 to 4 are considered in the analysis.

Based on the phase spectrum of the j-th decomposed component $\Phi_j(\omega)$, the group delay times $t_{gr}^{(j)}(\omega)$ at discrete frequencies within the compact support can be determined by Eq. (1), and then, the mean value $\mu_{tgr}^{(j)}$ and the standard deviation $\sigma_{tgr}^{(j)}$ of group delay times for the j-th decomposed component can be carried out. The distribution of group delay times for the decomposed components (j=-3 to 4) of the ground motion observed at station TCU052 is shown in Fig. 5, and the associated mean values and standard deviations are listed in Table 1.

In general, the group delay times and the associated mean value and standard deviation can be determined straightforwardly for each decomposed component of an observed ground motion, and the procedure is outlined in Fig. 6.

III. RANDOM GENERATION OF GROUP DELAY TIME FROM THE DISTRIBUTION CHARACTERISTIC

The histograms of the group delay times determined for each decomposed component with j=-1 to 4 of the ground motion observed at station TCU052 during the Chi-Chi earthquake are shown in Fig. 7. Compared with the density distribution functions of normal distribution and student t-distribution with a degree of freedom ϕ=3, it can be found that the t-distribution expresses well the probabilistic characteristic of group delay times. The density

Table 1 The mean value and the standard deviation of the group delay time

	$\mu_{tgr}^{(j)}$(sec)	$\sigma_{tgr}^{(j)}$(sec)
j=-3	44.5741	7.6745
j=-2	51.0558	8.8775
j=-1	45.3677	6.9164
j=0	43.4836	6.6704
j=1	51.1724	12.1331
j=2	47.9925	13.7978
j=3	45.6374	15.7368
j=4	45.7900	12.0596

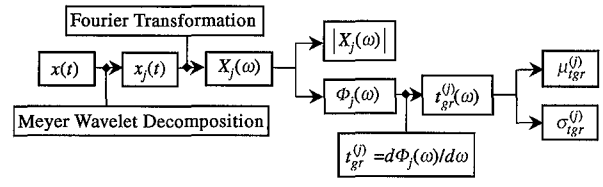

Fig. 6 Procedure to determine the group delay times and the associated mean value and standard deviation for each decomposed component of an observed ground motion

distribution function of the student t-distribution, with ϕ degrees of freedom of a random variable t, can be expressed by (Ang and Tang, 1975)

$$f_t(t) = \frac{\Gamma[(\phi+1)/2]}{\sqrt{\phi\pi}\cdot\Gamma(\phi/2)}\left(1+\frac{t^2}{\phi}\right)^{-\frac{\phi+1}{2}}$$

$$t = \frac{x-\mu}{(\sigma/\sqrt{\phi+1})} \tag{5}$$

herein, μ and σ are the mean and standard deviation of an independent random sample x.

In addition to the station TCU052, all of the ground motions observed at the stations in the central part of Taiwan during the Chi-Chi earthquake and its aftershock (M=6.8) are considered to study the probabilistic characteristic of group delay times. For the k-th observed ground motion (k=1~N, N: number of observed ground motions), the group delay time at each discrete frequency and the mean ($\mu_{tgr}^{(j)}$) and standard deviation ($\sigma_{tgr}^{(j)}$) for the j-th compact support (j= -1~4) can be determined straightforwardly by the procedures shown in Fig. 6. Furthermore, the probability density function $f_{obs}^{(j)}$ can be determined from the histograms of the observed group delay times within the j-th compact support. On the other hand, based on the determined $\mu_{tgr}^{(j)}$ and $\sigma_{tgr}^{(j)}$, the associated probability density function of the t-distribution, $f_{t,Eq(5)}^{(j)}(\phi)$, can be determined by Eq. (5) for a trial ϕ degrees of freedom. Based on the least squares method, the

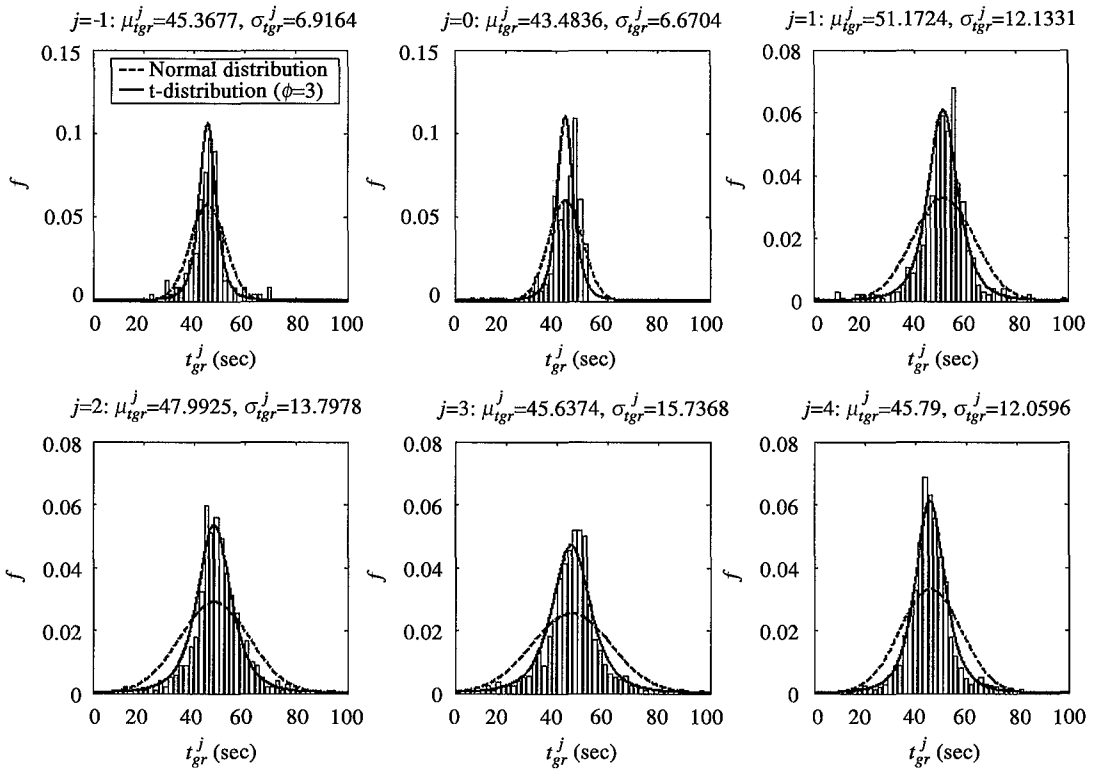

Fig. 7 Histograms of the group delay times determined for compact supports with j=-1 to 4 of the ground motion observed at station TCU052

ϕ-dependent error function can be defined by

$$Err(\phi) = \frac{1}{N}\sum_{k=1}^{N}\sum_{j=-1}^{4} w_j[f_{obs}^{(j)} - f_{t,Eq(5)}^{(j)}(\phi)]^2 \qquad (6)$$

Herein, w_j denotes the weighting that is defined by the bandwidth of the j-th compact support, and hence is proportional to the number of samples in the j-th compact support. It is noted that the ground motions observed at 73 stations for the main shock and 61 stations for the aftershock in the central part of Taiwan are analyzed. As shown in Fig. 8, the degree of freedom ϕ=3 causes the error function to become its minimum, for both the main shock and the aftershock. It implies that the student t-distribution, with a degree of freedom ϕ=3, can be recognized as the representative distribution of group delay times within a compact support for the central part of Taiwan. Hence, based on the means and standard deviations of the group delay times, the sample of group delay times at each discrete frequency within the bandwidth can be generated randomly by the identified student t-distribution (ϕ=3), and further, integrated to model the phase spectrum of design ground motions.

Consider the ground motion observed at station TCU052 during the Chi-Chi earthquake again, based

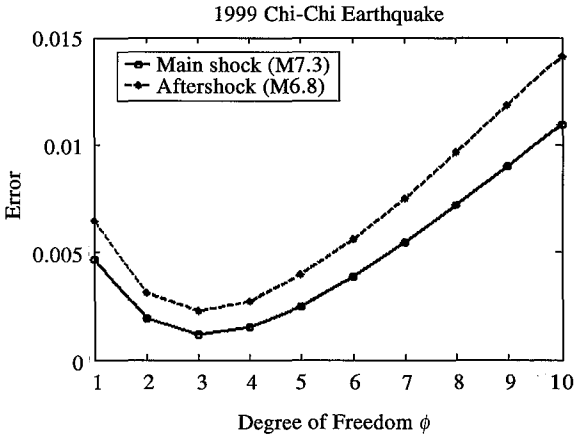

Fig. 8 ϕ-dependent error function determined by Eq. (6) for the main shock and the aftershock of the Chi-Chi earthquake

on the determined mean value ($\mu_{tgr}^{(j)}$) and standard deviation ($\sigma_{tgr}^{(j)}$), the sample of group delay times at each discrete frequency within the j-th compact support can be randomly generated by the identified student t-distribution (ϕ=3). Fig. 9 shows the comparison of the observed and randomly generated group delay times within the compact support with j=1 and 2. By integrating the randomly generated group delay times, the phase spectrum for the j-th component

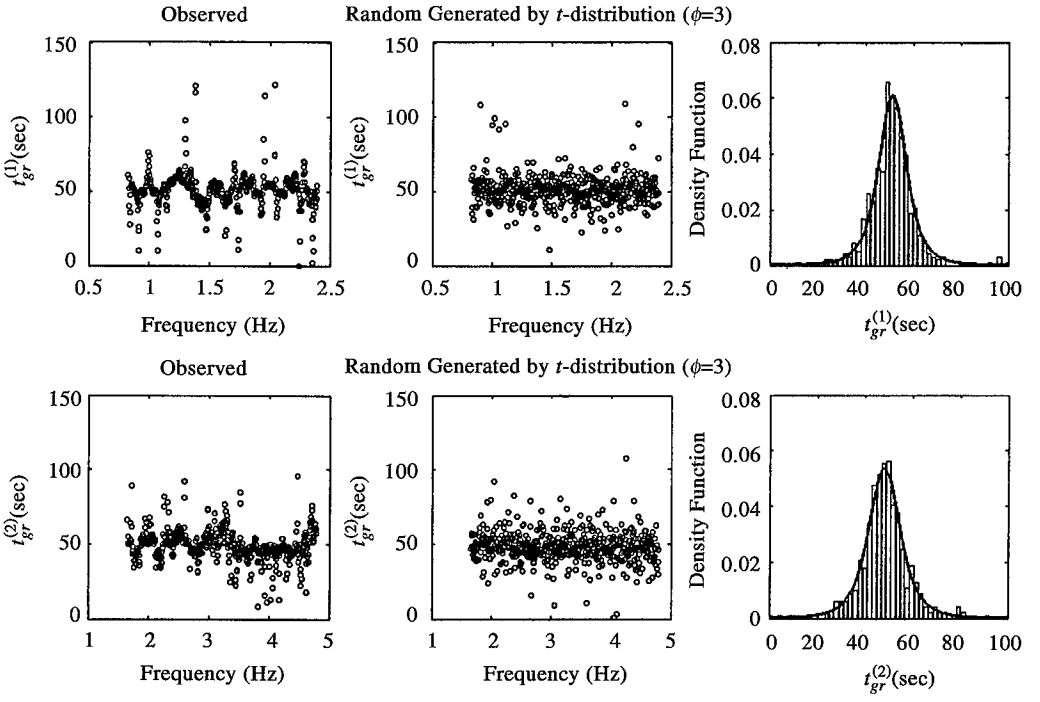

Fig. 9 Comparison of the observed and randomly generated group delay times within the compact support with j=1 and 2 of the components decomposed from the ground motion observed at station TCU052

can be simulated.

Combining the simulated phase spectrum and the forward-determined Fourier amplitude of each j-th component within its main frequency range ($2^{j-1} \leq f \leq 2^j$), the associated time history can be recovered by the inverse Fourier transformation. Fig. 10 shows the comparison of the recovered signal, denoted as a_{jr}, and the forward decomposed signal, denoted as a_{j0}, for each j-th component. It is found that they are in good agreement for lower frequency components. On the other hand, there exist significant differences for higher frequency components. It is because the separated groups with different arrival times can hardly be recovered by only one central arrival time ($\mu_{tgr}^{(j)}$). However, for a near-fault earthquake, the contribution due to the higher frequency components is less than that due to the lower frequency components. Therefore, the recovered total ground acceleration (summation of all of the j-th recovered components) is in good agreement with the original earthquake ground motion observed at TCU052 as shown in Fig. 11(a). Furthermore, the velocity pulse can also be recovered as shown in Fig. 11(b).

However, how to predict the mean value and the standard deviation of group delay times of each component at a site with no records available, and how to overcome the random numbers in generating the group delay times are not well defined yet, and these problems will be solved in the next section.

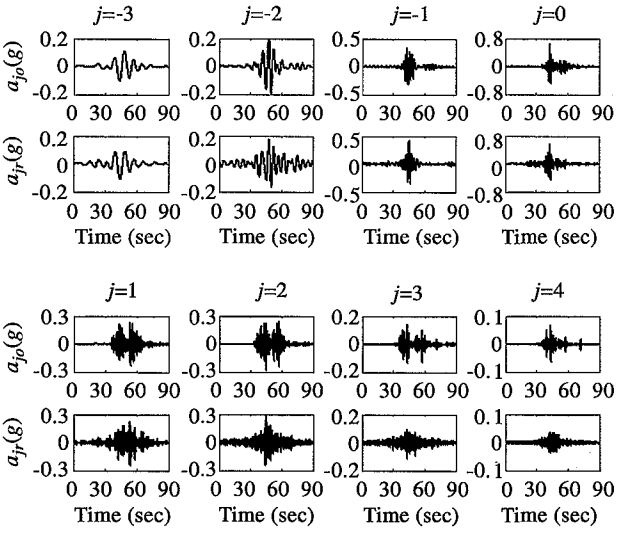

Fig. 10 Comparison of the recovered signals (denoted as a_{jr}) and the forward wavelet decomposed signals (denoted as a_{j0}) for the j-th component (j=-3 to 4) at station TCU052

IV. CONDITIONAL SIMULATION OF GROUP DELAY TIME AT AN UNOBSERVED SITE

In general, the mean value and standard deviation of group delay times of each component can be modeled as functions of the epicentral distance and earthquake magnitude. The parameters should be regressed by the observed earthquake data sets.

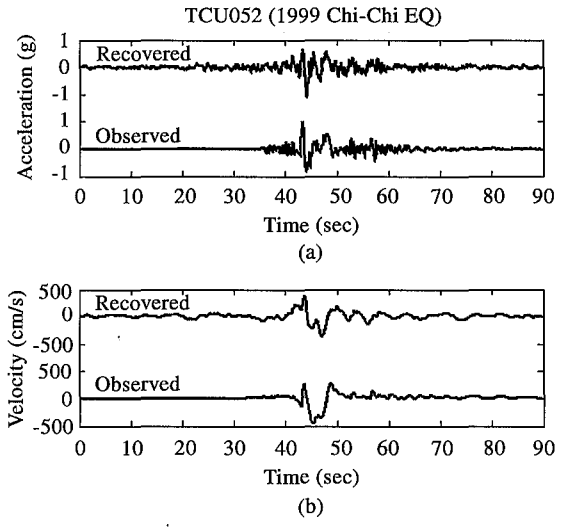

Fig. 11 Comparison of the observed and simulated total ground motion at station TCU052: (a) for ground acceleration and (b) for ground velocity

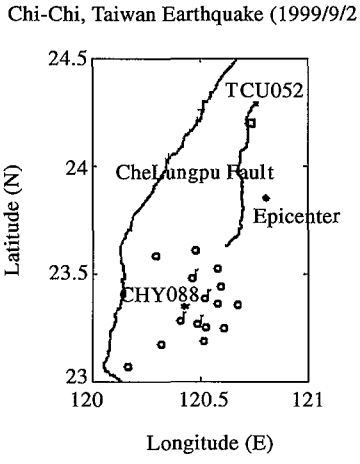

Fig. 12 Locations of the target site CHY088 and nearby observation stations

However, because the purpose of this study is to determine the design ground motion corresponding to the Chi-Chi earthquake at a site with no records available, the dependence of the earthquake magnitude can be dropped and only the earthquake data observed during the Chi-Chi earthquake are analyzed. The attenuation relations to predict the mean value $\mu_{tgr}^{(j)}$ and standard deviation $\sigma_{tgr}^{(j)}$ of group delay times of the j-th component are expressed as

$$\mu_{tgr}^{(j)}(R) = \alpha_1^{(j)} R^{\gamma_1^{(j)}}$$

$$\sigma_{tgr}^{(j)}(R) = \alpha_2^{(j)} R^{\gamma_2^{(j)}} \tag{7}$$

where R is the hypocentral distance and $\alpha_1^{(j)}$, $\alpha_2^{(j)}$, $\gamma_1^{(j)}$ and $\gamma_2^{(j)}$ are parameters to be determined by the regression analysis. It is noted that the recorded time sequence is relative to the trigger time of the accelerometer at each station when the detected ground acceleration exceeds a threshold. Therefore, the origin time of each observed time history should be synchronized to become the starting moment of the event by adding the calculated travel time of the direct P-wave generated at the hypocenter to the individual station trigger time.

In this paper, the station CHY088 is selected as the target site. The attenuation relations to predict the mean value $\mu_{tgr}^{(j)}$ and standard deviation $\sigma_{tgr}^{(j)}$ of group delay times are regressed by the earthquake data set recorded at the surrounding stations as denoted by open circles in Fig. 12. The regression results of the attenuation relations of the mean value and standard deviation are shown in Fig. 13, and the values of $\alpha_1^{(j)}$, $\alpha_2^{(j)}$, $\gamma_1^{(j)}$ and $\gamma_2^{(j)}$ are listed in Table 2.

Based on the regressed attenuation relations, the

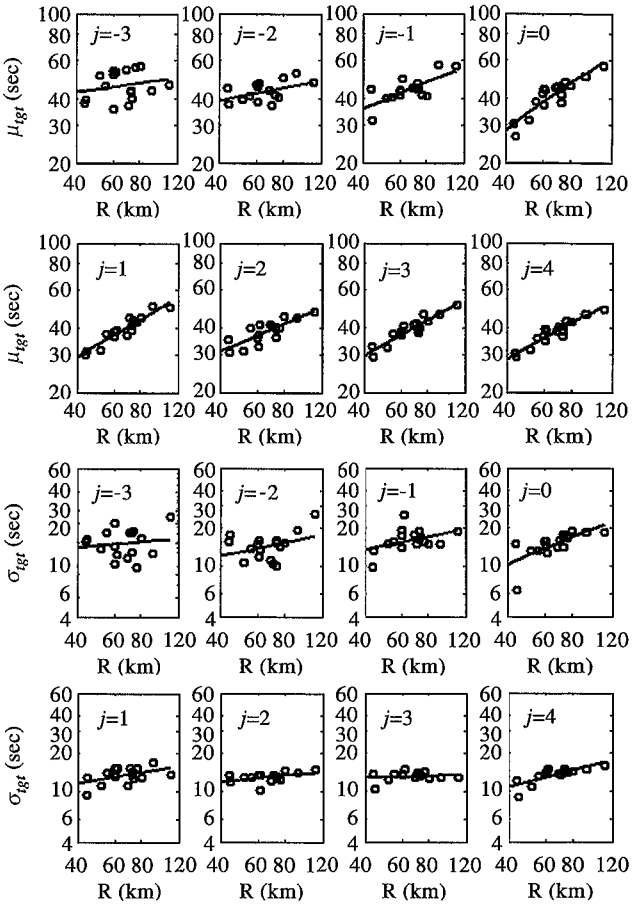

Fig. 13 Attenuation relations of the mean value $\mu_{tgr}^{(j)}$ and standard deviation $\sigma_{tgr}^{(j)}$ of group delay times

mean value and standard deviation of group delay times of each decomposed component at CHY088 can be predicted. Here, instead of random generation from only the predicted mean value and standard deviation by the identified student t-distribution

Table 2 Attenuation relations obtained from the regression analysis of the mean value ($\mu_{tgr}^{(j)}$) and the standard deviation ($\sigma_{tgr}^{(j)}$)

	$\mu_{tgr}^{(j)} = \alpha_1^{(j)} R^{\gamma_1^{(j)}}$		$\sigma_{tgr}^{(j)} = \alpha_2^{(j)} R^{\gamma_2^{(j)}}$	
	$\alpha_2^{(j)}$	$\gamma_1^{(j)}$	$\alpha_2^{(j)}$	$\gamma_2^{(j)}$
j=-3	26.57	0.131	9.31	0.177
j=-2	18.91	0.196	3.22	0.357
j=-1	7.86	0.411	3.73	0.349
j=0	1.92	0.730	0.70	0.729
j=1	3.34	0.588	4.01	0.289
j=2	6.28	0.432	6.49	0.167
j=3	3.97	0.546	9.94	0.068
j=4	3.64	0.559	2.07	0.448

(ϕ=3), the earthquake data observed at the nearby stations are included together to model the group delay times by applying the Kalman filtering technique. In this study, the four closest stations, with similar site conditions, around the target site (station CHY088) are selected, and the locations of these four nearby stations are denoted by open circles with superscripts 'r' in Fig. 12.

Consider m seismograms observed at m nearby stations with spatial coordinates X_p (p=1~m; m=4 in this study), the group delay time $t_{gr}^{(j)}(X_p, \omega_k)$ at X_p and a discrete circular frequency ω_k within the j-th compact support can be determined from the decomposed components. Then, the mean value $\mu_{tgr}^{(j)}(X_p)$ and standard deviation $\sigma_{tgr}^{(j)}(X_p)$ of each component at X_p can be determined straightforwardly. The spatial coordinate of the target site (station CHY088) is defined as X_{m+1}, and its mean value and standard deviation of group delay times predicted from Eq. (7) for the j-th component are denoted as $\mu_{tgr}^{(j)}(X_{m+1})$ and $\sigma_{tgr}^{(j)}(X_{m+1})$, respectively. To define the spatial correlation of group delay times, the covariance between any two points X_p and X_q (p,q,=1~m+1) are assumed as

$$M_{pq}^{(j)} = \sigma_{tgr}^{(j)}(X_p)\sigma_{tgr}^{(j)}(X_q)\exp(-\eta\Delta_{pq}) \tag{8}$$

where Δ_{pq} is the horizontal distance between X_p and X_q, and η is assumed to have a constant value of 0.1.

Defining a vector composed of the m+1 group delay times at X_p (p=1~m+1) and a certain circular frequency ω_k within the j-th compact support as

$$\boldsymbol{Z}^{(j)}(\omega_k) = \{t_{gr}^{(j)}(X_1, \omega_k)\ t_{gr}^{(j)}(X_2, \omega_k)\ \cdots\ t_{gr}^{(j)}(X_m, \omega_k)\ t_{gr}^{(j)}(X_{m+1}, \omega_k)\}^T \tag{9}$$

The mean and covariance matrix associated with $\boldsymbol{Z}^{(j)}(\omega_k)$ within the compact support can be expressed as

$$\overline{\boldsymbol{Z}}^{(j)} = \{\mu_{tgr}^{(j)}(X_1)\ \mu_{tgr}^{(j)}(X_2)\ \cdots\ \mu_{tgr}^{(j)}(X_m)\ \mu_{tgr}^{(j)}(X_{m+1})\}^T$$

$$\boldsymbol{M}^{(j)} = [M_{pq}^{(j)}(X_p, X_q)] \tag{10}$$

It is noted that all the values of the components in the mean vector $\overline{\boldsymbol{Z}}^{(j)}$ and the covariance matrix $\boldsymbol{M}^{(j)}$ can be well determined, as mentioned before. For the m observation points, the m-dimensional vector composed of the group delay times at ω_k can be defined as

$$\boldsymbol{y}^{(j)}(\omega_k) = \{t_{gr}^{(j)}(X_1, \omega_k)\ t_{gr}^{(j)}(X_2, \omega_k)\ \cdots\ t_{gr}^{(j)}(X_m, \omega_k)\}^T \tag{11}$$

According to Eqs. (9) and (11), it yields the observation equation

$$\boldsymbol{y}^{(j)}(\omega_k) = \boldsymbol{H}\boldsymbol{Z}^{(j)}(\omega_k) \quad \boldsymbol{H} = [\boldsymbol{I}\ \ 0] \tag{12}$$

where $\boldsymbol{H}$ is the observation matrix with a dimension of $m\times(m+1)$, and $\boldsymbol{I}$ is the unit matrix of order m.

The Kalman filtering technique is adopted to obtain the posterior best estimator of group delay times conditioned by the observation equation. Because the *apriori* best estimator and its covariance matrix are given by Eq. (10), the posterior best estimator of group delay times and the associated covariance matrix, denoted as $\hat{\boldsymbol{Z}}^{(j)}(\omega_k)$ and $\hat{\boldsymbol{M}}^{(j)}$, are expressed as

$$\hat{\boldsymbol{Z}}^{(j)}(\omega_k) = \overline{\boldsymbol{Z}}^{(j)} + \boldsymbol{K}^{(j)}(\boldsymbol{y}^{(j)}(\omega_k) - \boldsymbol{H}\overline{\boldsymbol{Z}}^{(j)})$$

$$\hat{\boldsymbol{M}}^{(j)} = \boldsymbol{M}^{(j)} - \boldsymbol{K}^{(j)}\boldsymbol{H}\boldsymbol{M}^{(j)} \tag{13}$$

where the matrix $\boldsymbol{K}^{(j)}$ with a dimension of $(m+1)\times m$ is the Kalman gain of the j-th component, and is defined as

$$\boldsymbol{K}^{(j)} = \boldsymbol{M}^{(j)}\boldsymbol{H}^T[\boldsymbol{H}\boldsymbol{M}^{(j)}\boldsymbol{H}^T + \boldsymbol{R}^{(j)}]^{-1} \tag{14}$$

The observation noise matrix $\boldsymbol{R}^{(j)}$ is assumed to be the zero matrix as the posterior best estimator of group delay times is approached. Partitioning the covariance matrix $\boldsymbol{M}^{(j)}$ into the observed and unobserved parts

$$\boldsymbol{M}^{(j)} = \begin{bmatrix} \boldsymbol{M}_{m,m}^{(j)} & \boldsymbol{M}_{m,m+1}^{(j)} \\ \boldsymbol{M}_{m+1,m}^{(j)} & \boldsymbol{M}_{m+1,m+1}^{(j)} \end{bmatrix} \tag{15}$$

and substituting Eq. (15) and the observation matrix $\boldsymbol{H}$ given in Eq. (12) into Eqs. (13) and (14), the Kalman gain $\boldsymbol{K}^{(j)}$, the posterior best estimators of group delay times $\hat{\boldsymbol{Z}}^{(j)}(k)$ and its covariance matrix

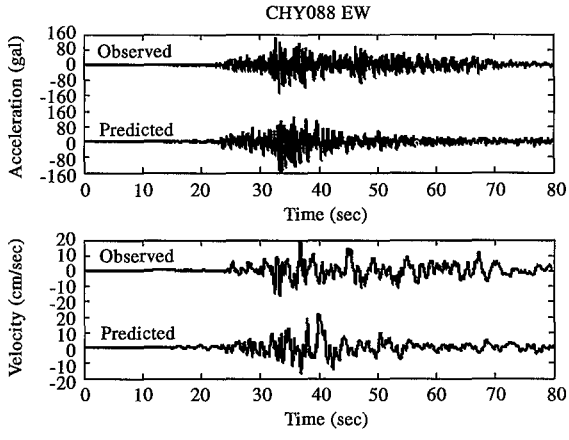

Fig. 14 Comparison of the observed and predicted total ground motion at the target site CHY088

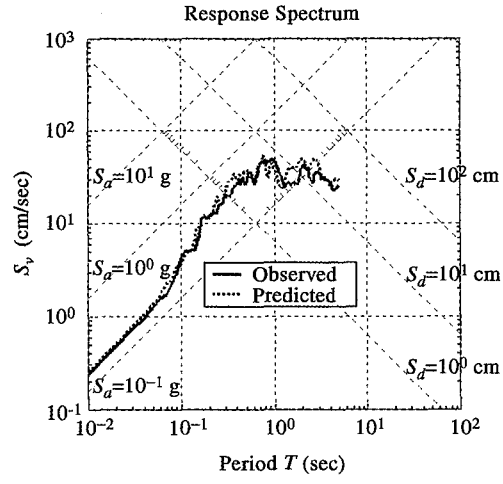

Fig. 15 Comparison of the response spectra associated with the observed and predicted ground motions at the target site CHY088

$\boldsymbol{M}^{(j)}$ can be determined under the condition of $\boldsymbol{R}^{(j)}=0$ as

$$\boldsymbol{K}^{(j)}=\begin{bmatrix} \boldsymbol{I} \\ \boldsymbol{M}^{(j)}_{m+1,m}(\boldsymbol{M}^{(j)}_{m,m})^{-1} \end{bmatrix} \tag{16}$$

$$\hat{\boldsymbol{Z}}^{(j)}(\omega_k)=\begin{Bmatrix} \hat{\boldsymbol{Z}}^{(j)}_m(\omega_k) \\ \hat{\boldsymbol{Z}}^{(j)}_{m+1}(\omega_k) \end{Bmatrix}$$

$$=\begin{Bmatrix} \boldsymbol{y}^{(j)}(\omega_k) \\ \overline{\boldsymbol{Z}}^{(j)}_{m+1}+\boldsymbol{M}^{(j)}_{m+1,m}(\boldsymbol{M}^{(j)}_{m,m})^{-1}(\boldsymbol{y}^{(j)}(\omega_k)-\overline{\boldsymbol{Z}}^{(j)}_m) \end{Bmatrix} \tag{17}$$

$$\hat{\boldsymbol{M}}^{(j)}=\begin{bmatrix} 0 & 0 \\ 0 & \boldsymbol{M}^{(j)}_{m+1,m+1}-\boldsymbol{M}^{(j)}_{m+1,m}(\boldsymbol{M}^{(j)}_{m,m})^{-1}\boldsymbol{M}^{(j)}_{m,m+1} \end{bmatrix} \tag{18}$$

These results show that the posterior best estimators of group delay times at observation points are identical to the observed values and that the associated components of covariance matrix become zero. For the target site X_{m+1} (station CHY088), the posterior best estimator of group delay times at a discrete circular frequency ω_k within the j-th compact support ($2\pi 2^j/3\le\omega_k\le 2\pi 2^{j+2}/3$) can be summarized to be

$$\hat{t}^{(j)}_{gr}(X_{m+1},\omega_k)$$

$$=\mu^{(j)}_{tgr}(X_{m+1})+\boldsymbol{M}^{(j)}_{m+1,m}(\boldsymbol{M}^{(j)}_{m,m})^{-1}(\boldsymbol{y}^{(j)}(\omega_k)-\overline{\boldsymbol{Z}}^{(j)}_m) \tag{19}$$

Therefore, by integrating the simulated group delay times, the phase spectrum of each j-th component can be modeled within the compact support for the target site. Furthermore, considering the predicted phase spectrum and the forward-determined Fourier amplitude from the ground motion observed at station CHY088, the time history of the predicted ground motion can be recovered by the inverse Fourier transformation. The time histories of the acceleration and velocity between the observed and predicted signals are compared in Fig. 14. Fig. 15 shows the comparison of the response spectra associated with the observed and predicted ground motions by a 4-way logarithm format, and it can be seen that they are in good agreement.

V. SPECTRUM COMPATIBLE DESIGN GROUND MOTION

Based on the regressed attenuation relations, the mean value and standard deviation of group delay times for each component at a site of interest can be predicted. Then, the sample of group delay times can be either generated randomly by the identified student t-distribution (ϕ=3), or simulated conditionally by applying the Kalman filtering technique to consist of the earthquake data observed at nearby stations. Finally, the phase spectrum can be determined by integrating the group delay time within the non-overlapped main frequency range ($2^{j-1}\le f\le 2^j$) of each j-th compact support. The procedure to model the phase spectrum for a target site is outlined in Fig. 16. On the other hand, in addition to the modeling of phase spectrum for a target site, the Fourier amplitude should be determined to simulate the design ground

Table 3 Code-defined normalized response spectrum coefficients for soil profile type III

Period Range(sec)	Extremely Short $T\leq0.03$	Very Short $0.03\leq T\leq0.2$	Short $0.2\leq T\leq0.611$	Moderate $0.611\leq T\leq2.415$	Long $T\geq2.415$
$S_{aD}(T)$	1.0	$8.824T+0.7352$	2.5	$1.8/T^{2/3}$	1.0

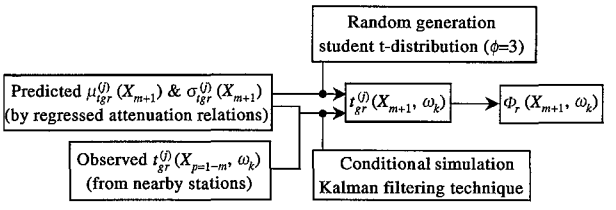

Fig. 16 Procedure to model the phase spectrum from the group delay times predicted by either the student t-distribution (ϕ=3) or the Kalman filtering technique

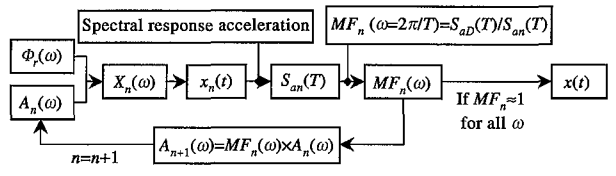

Fig. 17 Procedure to determine the ground motion compatible with the design spectral response acceleration

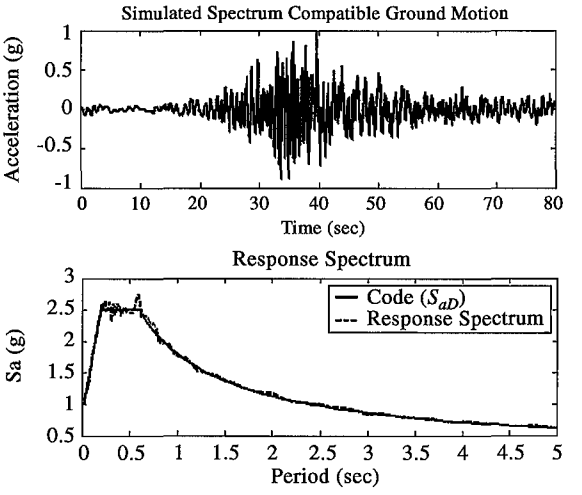

Fig. 18 Spectrum compatible ground motion at the target site CHY088

motion, such that the associated spectral response acceleration will be compatible with the design response spectrum as specified by the seismic design code.

The procedure to simulate a ground motion compatible with the expected design spectrum is illustrated in Fig. 17. Based on the modeled phase spectrum $\Phi_r(\omega)$ and a trial Fourier amplitude $A_n(\omega)$, we can recover the total ground motion, and then determine the associated spectral acceleration $S_{an}(T)$ for any structural period T. Because the response is dominated by the wave with resonant frequency, the modification factor for the Fourier amplitude at a circular frequency of $\omega=2\pi/T$ can be defined by

$$MF_n(\omega)|_{\omega=2\pi/T}=S_{aD}(T)/S_{an}(T) \tag{20}$$

where $S_{aD}(T)$ is the normalized design spectral response acceleration for a structure with period T. Then the Fourier amplitude on the next iteration process can be defined by

$$A_{n+1}(\omega)=MF_n(\omega)\times A_n(\omega) \tag{21}$$

We repeat this iteration process until $MF_n(\omega)$ is equal to 1.0 at all frequencies.

It is noted that station CHY088 is located on a soft site, thus, the normalized design spectral response acceleration $S_{aD}(T)$ specified by the current seismic design code in Taiwan for Soil Profile Type III (Soft Soil) should be considered. The associated values of $S_{aD}(T)$ are listed in Table 3. Based on the predicted phase spectrum for the target site (CHY088) and the procedure shown in Fig. 17, the spectrum compatible ground motion can be simulated and shown in Fig. 18. Furthermore, consider the zoning factor Z=0.33g at the target site, which means the design PGA corresponding to a return period of 475 years as specified by the current seismic design code in Taiwan, the simulated spectrum compatible ground motion can be scaled to have a peak ground acceleration of 0.33g to become the design ground motion at the target site (CHY088), and further, can be applied as the input ground motion to analyze the earthquake performance of structures for design purposes.

VI. CONCLUSIONS

Based on the ground motions observed during the Chi-Chi earthquake, the attenuation relations to predict the mean value and standard deviation of group delay times within each frequency range according to the compact support of Meyer wavelet can be regressed as functions of the hypocentral distance.

Based on the predicted mean value and standard deviation at a site of interest, the sample of group delay times can be generated randomly by the identified student t-distribution (ϕ=3). In addition to random generation, the sample of group delay times can be also simulated conditionally from the predicted mean value and standard deviation as well as the earthquake data observed at nearby stations by applying the Kalman filtering technique. Then, the phase spectrum at a site of interest can be modeled by integrating the simulated group delay times. Finally, owing to the resonance effect, the Fourier amplitude can be modified by forcing the associated spectral response acceleration to be compatible with the design response spectrum as specified by the seismic design code. Therefore, based on the predicted phase spectrum and the modified Fourier amplitude, the design ground motion at a site with no records available can be simulated. The simulated design ground motion will be compatible with the design response spectrum and also perform the same waveform characteristics as the earthquake ground motions observed at the target site. Hence, the time history analysis can be implemented to analyze the earthquake performance for design purposes.

ACKNOWLEDGEMENTS

The authors gratefully thank the Central Weather Bureau in Taiwan for their kindness in providing the strong ground motion data recorded during the Chi-Chi earthquake.

REFERENCES

1. Ang, A. H-S, and Tang, W. H., 1975, *Probability Concepts in Engineering Planning and Design - Volume I Basic Principles*, John Wiley & Sons, New York.
2. Daubechies, I., 1992, *Ten Lectures on wavelets*, Volume 61 of CBMSNSF Regional Conference Series in Applied Mathematics, SIAM Press, Philadelphia, Pennsylvania.
3. Hoshiya, M., and Murayama, O., 1993, "Stochastic Interpolation of Earthquake Wave Propagation," *Proceedings of the 6th International Conference on Structural Safety and Reliability*, Innsbruck.
4. Jennings, P. C., Housner, G. W., and Tstai, N. C., 1968, "Simulated Earthquake Motions for Design Purpose," *Proceedings of the 4th World Conference on Earthquake Engineering*, pp. 145-160.
5. Kameda, H., and Morikawa, H., 1992, "An Interpolating Stochastic Process for Simulation of Conditional Random Fields," *Probabilistic Engineering Mechanics*, Vol. 7, No. 4, pp. 243-254.
6. Meyer, Y., 1989, "Orthonormal Wavelets," In *Wavelets*, Springer, pp. 21-27.
7. Papoulis, A., 1962, *The Fourier Integral and Its* Application, McGraw-Hill, New York.
8. Sato, T., Murono, Y., and Nishimura, A., 1998, "A Method to Estimate Phase Spectrum Taking into Account Source, Path and Site Effects," *Proceedings of the 11th European Conference on Earthquake En-gineering.*
9. Sato, T., Murono, Y., and Nishimura, A., 1999, "Modeling of Phase Spectrum to Simulate Design Earthquake Motion," *Optimizing Post-Earthquake Lifeline System Reliability*, W.M. Elliot and P. McDonough, eds., Technical Council on Lifeline Earthquake Eng., ASCE, Monograph No. 16, pp. 804-813.
10. Sato, T., and Imabayashi, H,. 1999, "Real Time Conditional Simulation of Earthquake Ground Motion," *Earthquake Engineering and Engineering Seismology*, Vol. 1, No. 1, 27-38.
11. Satoh, T., Uetake, T., and Sugawara, Y., 1996, "A Study on Envelope Characteristics of Strong Motions in a Period Range of 1 to 15 Seconds by Using Group Delay Time," *Proceedings of the 11th World Conference on Earthquake Engineering*, Paper No. 149.
12. Shinozuka, M., and Jan, C.-M., 1972, "Digital Simulation of Random Processes and Its Applications," *Journal of Sound and Vibration*, Vol. 25, No. 1, pp. 111-128.
13. Vanmarck, E. H., and Fenton, G. A., 1991, "Conditional Simulation of Local Fields of Earthquake Ground Motion," *Journal of Structural Safety*, Vol. 10, pp. 247-264.

Manuscript Received: Dec. 11, 2001
Revision Received: May 08, 2002
and Accepted: May 21, 2002

相位頻譜模擬與設計地表運動歷時

柴駿甫　羅俊雄

國家地震工程研究中心

佐藤忠信

日本京都大學防災研究所

摘　要

本文藉由小波轉換與逆轉換公式，計算地表運動歷時於特定頻寬範圍內各離散頻率之群延遲時間以及於此頻寬範圍內的平均值與標準差，並藉由統計回歸方式，求得平均值與標準差隨震央距變化的經驗公式。故針對某一地震事件的特殊場址，可估算其群延遲時間於特定頻寬範圍之平均值與標準差。藉由此估算之平均值與標準差，配合群延遲時間的t-分佈特性，可隨機產生一組分佈於該頻寬範圍內各離散點的群延遲時間。另一方面，藉由 Kalman 濾波技術之條件模擬方法，可結合該特殊場址附近的實測地震記錄，求得各離散頻率的群延遲時間。藉由模擬之群延遲時間，可進而積分得該頻寬範圍內的相位頻譜。同時，配合設計反應譜，可修正其傅立葉震幅譜，獲致滿足場址地表運動特性並與設計反應譜相容的地表運動歷時，作爲結構物地震行爲分析之依據。

關鍵詞：相位頻譜，群延遲時間，設計反應譜， Kalman 濾波技術。